

GITT studies on oxide cathode $\text{LiNi}_{1/3}\text{Co}_{1/3}\text{Mn}_{1/3}\text{O}_2$ synthesized by citric acid assisted high-energy ball milling

WEIDONG ZHENG, MIAO SHUI*, JIE SHU, SHAN GAO, DAN XU, LIANGLIANG CHEN, LIN FENG and YUANLONG REN

The State Key Laboratory Base of Novel Functional Materials and Preparation Science; The Faculty of Materials Science and Chemical Engineering, Ningbo University, Ningbo 315211, P. R. China

MS received 19 April 2012; revised 3 July 2012

Abstract. Layered $\text{LiNi}_{1/3}\text{Co}_{1/3}\text{Mn}_{1/3}\text{O}_2$ was synthesized by a citric acid assisted solid-state method. The structure and electrochemical properties of the $\text{LiNi}_{1/3}\text{Co}_{1/3}\text{Mn}_{1/3}\text{O}_2$ materials were investigated. XRD analysis indicated the as-synthesized $\text{LiNi}_{1/3}\text{Co}_{1/3}\text{Mn}_{1/3}\text{O}_2$ was with the layered $\alpha\text{-NaFeO}_2$ structure. The discharge capacity was about $154 \text{ m}\cdot\text{Ahg}^{-1}$ at $0.1 \text{ }^\circ\text{C}$ rate in the range of 2.0–4.5 V. The kinetics of the $\text{LiNi}_{1/3}\text{Co}_{1/3}\text{Mn}_{1/3}\text{O}_2$ materials was investigated by the galvanostatic intermittent titration technique (GITT) method. The lithium ion diffusion coefficient of the $\text{LiNi}_{1/3}\text{Co}_{1/3}\text{Mn}_{1/3}\text{O}_2$ was determined in the range of 10^{-8} – $10^{-9} \text{ cm}^2\cdot\text{s}^{-1}$ as a function of voltage of 3.7–4.5 V.

Keywords. Li diffusion; $\text{LiNi}_{1/3}\text{Co}_{1/3}\text{Mn}_{1/3}\text{O}_2$; lithium ion batteries; layered structure.

1. Introduction

In the past two decades, the popularization of diverse portable devices has motivated a large group of researchers devoted to lithium-ion batteries study, especially the cathode materials. Among them, the LiCoO_2 has dominated the cathode material market since it was first commercialized by Sony Corporation in 1990. For the high cost and toxicity of cobalt, the layered $\alpha\text{-NaFeO}_2$ structure LiCoO_2 derived transition metal oxides $\text{Li}_{1+y}\text{Ni}_x\text{Co}_{1-2x}\text{Mn}_x\text{O}_2$ (Shaju and Bruce 2006), the spinel LiMn_2O_4 (Lee *et al* 2001) and the olivine LiFePO_4 (Lim *et al* 2008) have attracted much attention as alternative to LiCoO_2 , especially with the advent of the hybrid electric car. The layered $\text{Li}_{1+y}\text{Ni}_x\text{Co}_{1-2x}\text{Mn}_x\text{O}_2$ stands out for its higher plateau voltage, better rate performance and thermal stability (Shaju and Bruce 2006). Furthermore, it is believed that they have a superior diffusion pathway of two dimensions to the spinel LiMn_2O_4 of three dimensions and the olivine LiFePO_4 of one dimension (Chuying *et al* 2007). Recently the layered $\text{LiNi}_{1/3}\text{Co}_{1/3}\text{Mn}_{1/3}\text{O}_2$ prepared by Peter G Bruce group (Shaju and Bruce 2006) exhibits an excellent capacity and rate performance to be the potential cathode material for the next-generation lithium-ion batteries. Before the large-scale application for high-power batteries, kinetics of the lithium ion intercalation in cathode materials shall be scrutinized, which basically determines the rate at which the battery can be charged and discharged. Although the investigations of lithium intercalation–deintercalation mechanism for $\text{Li}_{1-y}\text{Ni}_{1/3}\text{Mn}_{1/3}\text{Co}_{1/3}\text{O}_2$ were carried out (Kobayashi

et al 2005), the lithium ion diffusion kinetics were not fully covered yet, especially by the method of galvanostatic intermittent titration technique (GITT).

In this paper, we focused on the diffusion kinetics of the $\text{LiNi}_{1/3}\text{Co}_{1/3}\text{Mn}_{1/3}\text{O}_2$ cathode materials prepared by the citric acid assisted solid-state method. The structural and electrochemical performance were characterized. The lithium ion diffusion coefficients of $\text{LiNi}_{1/3}\text{Co}_{1/3}\text{Mn}_{1/3}\text{O}_2$ material as a function of voltage determined by GITT method were fully discussed.

2. Experimental

2.1 Preparation of $\text{LiNi}_{1/3}\text{Co}_{1/3}\text{Mn}_{1/3}\text{O}_2$

$\text{LiNi}_{1/3}\text{Co}_{1/3}\text{Mn}_{1/3}\text{O}_2$ used for GITT measurement was synthesized by solid-state method as follows: lithium acetate dihydrate ($\text{C}_2\text{H}_7\text{LiO}_4$), nickel(II) acetate tetrahydrate ($\text{C}_4\text{H}_6\text{NiO}_4\cdot 4\text{H}_2\text{O}$), manganese(II) acetate tetrahydrate ($\text{C}_4\text{H}_6\text{MnO}_4\cdot 4\text{H}_2\text{O}$) and cobalt(II) acetate tetrahydrate ($\text{C}_4\text{H}_6\text{CoO}_4\cdot 4\text{H}_2\text{O}$) were used as raw materials. A stoichiometric amount of $\text{C}_2\text{H}_7\text{LiO}_4$, $\text{C}_4\text{H}_6\text{NiO}_4\cdot 4\text{H}_2\text{O}$, $\text{C}_4\text{H}_6\text{MnO}_4\cdot 4\text{H}_2\text{O}$ and $\text{C}_4\text{H}_6\text{CoO}_4\cdot 4\text{H}_2\text{O}$ (molar ratio of Li:Ni:Co:Mn was 3:1:1:1) were ball-milled for 10 h with appropriate amount of anhydrous ethanol and citric acid as mediator. After drying for 6 h at $80 \text{ }^\circ\text{C}$, the fluffy mixture was obtained. Then the mixture was ground before calcination at $920 \text{ }^\circ\text{C}$ for 10 h with a rate of $5 \text{ }^\circ\text{C}\cdot\text{min}^{-1}$. All the experiments were carried out at an ambient atmosphere and all the raw materials were of analytical grade purchased from Sino-pharm Chemical Reagent Co. Ltd.

* Author for correspondence (shuimiao@nbu.edu.cn)

2.2 Characterization of $\text{LiNi}_{1/3}\text{Co}_{1/3}\text{Mn}_{1/3}\text{O}_2$

The structure of the as-synthesized sample was identified by X-ray diffractometer Bruker AXS D8 FOCUS using $\text{CuK}\alpha$ radiation from $2\theta = 15$ to 75° operated at 36 kV and 20 mA.

The coin-type cell CR2012 consisting of a metallic-lithium foil anode separated by Celgard 2300 polypropylene membrane was fabricated in a glove box filled with high pure argon. The cathode was prepared from a paste by mixing the as-synthesized sample, the conductive acetylene black and the polyvinylidene fluoride (PVDF) binder with a mass ratio of 4:1:1 in NMP solvent. The paste was coated on the aluminum foil and then dried at 120°C for 10 h under vacuum before the cell was assembled. The electrolyte was 1 M LiPF_6 dissolved in the mixture of EC and DMC (V:V = 1:1) solution. All the cells were aged for 24 h before electrochemical testing. Prior to the galvanostatic intermittent titration technique (GITT) measurement, the cell was charged and discharged for 10 cycles to make the electrode/electrolyte interface reach stable state. The charge–discharge tests were carried out on the multi-channel land battery testing system with the voltage ranging from 2.0 to 4.5 V. Here 160 mA h g^{-1} was assumed to be roughly equivalent to the 1C of the sample. For the GITT measurement, the cells were charged at a current of 0.2 mA for 200 s followed by an open circuit relaxation for 1 h. The procedure was continued until the voltage reached the required value. All the electrochemical testing were conducted at room temperature at about 25°C .

3. Results and discussion

Figure 1 shows XRD patterns of the as-synthesized $\text{LiNi}_{1/3}\text{Co}_{1/3}\text{Mn}_{1/3}\text{O}_2$ sample. All the diffraction positions can be indexed to the hexagonal $\alpha\text{-NaFeO}_2$ structure ($R\text{-}3m$ space group) without the evidence of impurity secondary phase. In the XRD patterns, the splits of (006)/(102) and (108)/(110) doublets are observed, indicating that the layered $\text{LiNi}_{1/3}\text{Co}_{1/3}\text{Mn}_{1/3}\text{O}_2$ cathode material

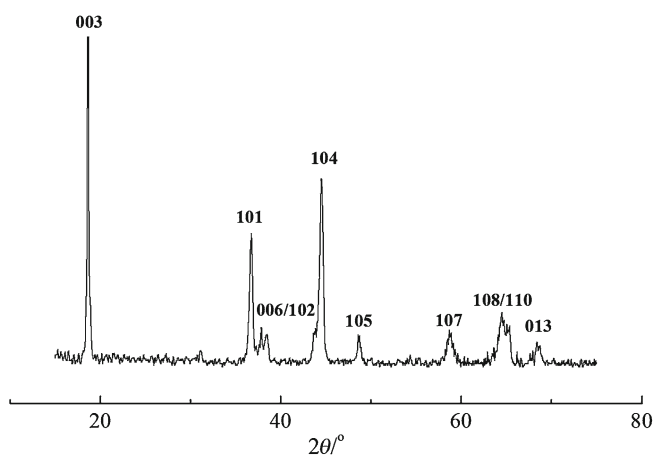


Figure 1. XRD patterns of $\text{LiNi}_{1/3}\text{Co}_{1/3}\text{Mn}_{1/3}\text{O}_2$ samples.

has been successfully synthesized. The lattice parameters and other structural parameters calculated based on XRD results for $\text{LiNi}_{1/3}\text{Co}_{1/3}\text{Mn}_{1/3}\text{O}_2$ are summarized in table 1. Some researchers used the high-integrated intensity ratio of the I_{003}/I_{104} to indicate the cation mixing of the layered structure, which is supposed to be a key factor influencing the electrochemical performance of layered $\text{LiNi}_{1/3}\text{Co}_{1/3}\text{Mn}_{1/3}\text{O}_2$ materials. Generally, when $I_{003}/I_{104} > 1.2$, the cation mixing is small with good layered structure. Here in this work, the I_{003}/I_{104} value is far larger than 1.2 indicating no undesirable cation mixing takes place. The lattice parameter, a , which is related to average metal–metal intra-slab distance, the lattice parameter, c , which is correlated to the average metal–metal inter-slab distance, the trigonal distortion, c/a and the cell volume, V are in good agreement with the literature (Li *et al* 2010b). In addition, R -factor ($R = (I_{102} + I_{006})/I_{101}$) is believed to be an indicator of hexagonal ordering, the lower the R -factor, the better the hexagonal ordering. It can be seen from table 1 that the synthesized $\text{LiNi}_{1/3}\text{Co}_{1/3}\text{Mn}_{1/3}\text{O}_2$ has a relatively low R -factor of 0.489. The test cells are operated at a constant current density of 0.1C rate between 2.6 and 4.5 V vs Li at room temperature. Figure 2 shows first, second, third, 49th and 50th charge/discharge curve of $\text{LiNi}_{1/3}\text{Co}_{1/3}\text{Mn}_{1/3}\text{O}_2$ powder. Figure 3 illustrates cycling performance of $\text{LiNi}_{1/3}\text{Co}_{1/3}\text{Mn}_{1/3}\text{O}_2$ material up to 50 cycles. From the figure, the test cell shows quite smooth and monotonous charge/discharge curves. On charging, the voltage sharply rises to 3.7 V, then slowly and monotonously increases to 4.5 V. The initial charge

Table 1. Calculated structure parameters for $\text{LiNi}_{1/3}\text{Co}_{1/3}\text{Mn}_{1/3}\text{O}_2$.

$a/\text{\AA}$	$c/\text{\AA}$	c/a	Cell volume/ \AA^3	I_{003}/I_{104}	$I = (I_{102} + I_{006})/I_{101}$
2.855	14.224	4.982	100.37	2.390	0.489

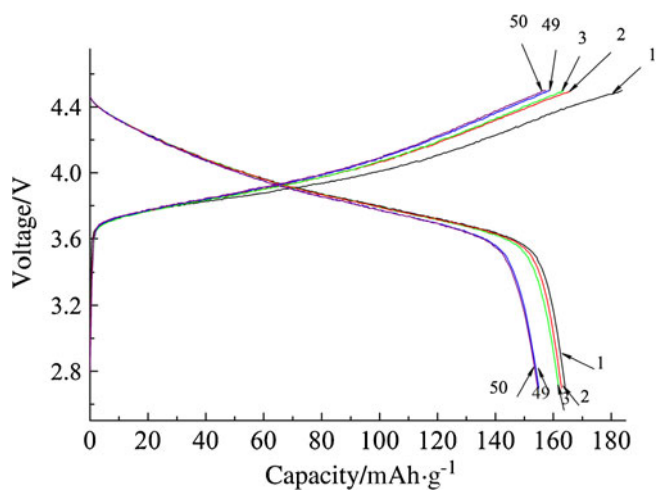


Figure 2. Charge–discharge curves of $\text{LiNi}_{1/3}\text{Co}_{1/3}\text{Mn}_{1/3}\text{O}_2$ cathode material.

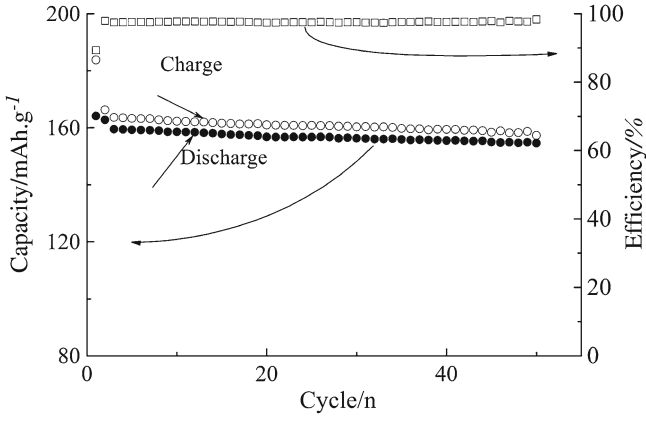


Figure 3. Cycling performance of $\text{LiNi}_{1/3}\text{Co}_{1/3}\text{Mn}_{1/3}\text{O}_2$ cathode material.

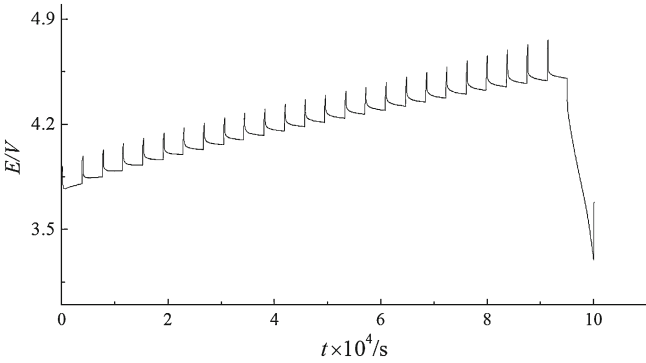


Figure 4. GITT curve of $\text{LiNi}_{1/3}\text{Co}_{1/3}\text{Mn}_{1/3}\text{O}_2$ cathode material.

capacity reaches $183 \text{ mAh}\cdot\text{g}^{-1}$ and discharge capacity $164 \text{ mAh}\cdot\text{g}^{-1}$ with an efficiency of 89%. A relatively large irreversible capacity loss is observed. However, for the following cycles, the charge/discharge capacities gradually stabilize between 154 and $164 \text{ mAh}\cdot\text{g}^{-1}$ and more than 97% discharge efficiency are observed. For the 50th cycle, a discharge capacity of $154.6 \text{ mAh}\cdot\text{g}^{-1}$ is still reserved with discharge capacity retention ratio of over 94%. In this work, $\text{LiNi}_{1/3}\text{Co}_{1/3}\text{Mn}_{1/3}\text{O}_2$ cathode material exhibits an excellent cycling performance, which is comparable to the method of co-precipitation reported in the literature (Luo *et al* 2006).

GITT measurement originally proposed by Wen *et al* (1979) is evaluated recently in the literature by Dess (2005). This measurement is based on the chrono-potentiometry and used as a standard method for the determination of the chemical diffusion coefficient of LiCoO_2 , LiNiO_2 , LiMn_2O_4 and LiFePO_4 (Li *et al* 2010a). Figure 4 shows GITT curve of $\text{LiNi}_{1/3}\text{Co}_{1/3}\text{Mn}_{1/3}\text{O}_2$ electrode after 10 cycles in the voltage range of 3.7–4.5 V. During the GITT measurement, the cell is charged at a constant current of 0.2 mA ($I_0 = 0.2 \text{ mA}$) for an intermittent 200 s followed by an open circuit relaxation of 1 h to reach the steady-state voltage (E_s). The procedure is continued until the cut-off voltage is reached. A single titration profile at around 3.77 V is illustrated in figure 5 with

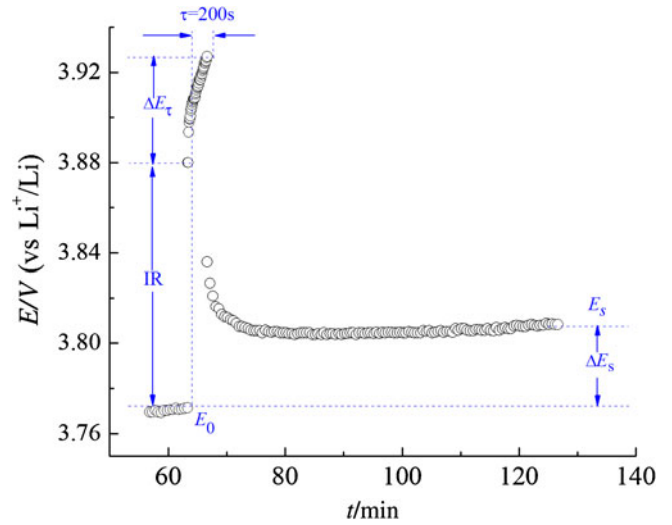


Figure 5. Scheme for a single step of a GITT experiment at around 3.77 V of $\text{LiNi}_{1/3}\text{Co}_{1/3}\text{Mn}_{1/3}\text{O}_2$ cathode material.

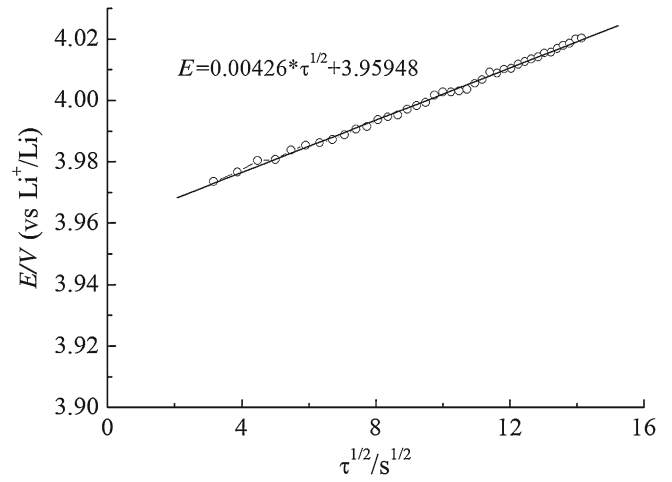


Figure 6. Variation of cell voltage during single titration plotted against $\tau^{1/2}$ to show linear fit.

schematic labelling parameters. As shown in figure 5, the change in the steady-state voltage ΔE_s is obtained by subtracting the original voltage (E_0) from the steady-state voltage (E_s). The process of the chemical diffusion is assumed to obey Fick's second law of diffusion. With a series of simplifications, for sufficient time interval ($\tau \ll L^2/D_{\text{Li}^+}$), the equation of D_{Li^+} can be written as:

$$D_{\text{Li}^+} = \frac{4}{\pi} \left(\frac{m_B V_M}{M_B S} \right)^2 \times \left(\frac{\Delta E_s}{\tau (dE_\tau/d\sqrt{\tau})} \right)^2 \quad (\tau \ll L^2/D_{\text{Li}^+}), \quad (1)$$

where m_B , M_B , V_M are mass, molecular weight and molar volume of $\text{LiNi}_{1/3}\text{Co}_{1/3}\text{Mn}_{1/3}\text{O}_2$, L and S are the thickness of the electrode and the overall contact area of the electrode and the electrolyte. As shown in figure 6,

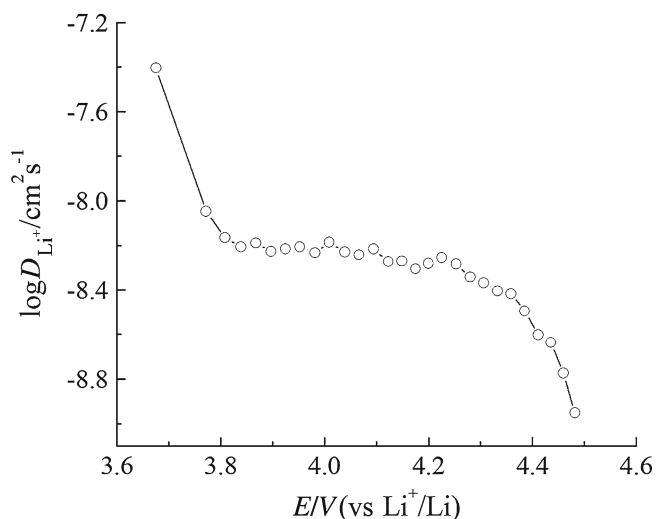


Figure 7. Chemical diffusion coefficient of Li⁺ as a function of voltage calculated by GITT.

the voltage shows a linear behaviour with the square root of τ . Therefore (1) can be further simplified as:

$$D_{\text{Li}^+} = \frac{4L^2}{\pi\tau} \left(\frac{\Delta E_s}{\Delta E_\tau} \right)^2 \quad (\tau \ll L^2/D_{\text{Li}^+}). \quad (2)$$

Based on (2), the chemical diffusion coefficients of Li⁺ calculated from GITT as a function of cell voltage are plotted in figure 7. It can be seen that, the lithium-ion chemical diffusion coefficients in LiNi_{1/3}Co_{1/3}Mn_{1/3}O₂ composite electrode vary from 10⁻⁸ to 10⁻⁹ cm²·s⁻¹ in the voltage range of 3.7–4.5 V. The curve of the chemical diffusion coefficients exhibits a twisting downtrend. At voltage of 3.7 V, value of the chemical diffusion coefficient is maximum in accordance with the sharp increase in the voltage of the charging curve in figure 2. Then the value decreases slowly with the increasing voltage until the upper cut-off voltage is reached. This tendency is in correspondence with the lithium-ion diffusion mechanisms in the layered intercalation compounds in terms of first-principle method by Van der Ven and Ceder (2001). The lithium ion diffusion coefficient varies two orders of magnitude with the voltage of the test cell, which determines the concentration of the divacancy and the activation barrier for lithium ion diffusion. With a low concentration of lithium ion in the cathode, viz. a high voltage of the cell, the concentration of the divacancy turns low and the activation barrier for diffusion increases, both resulting in a decrease in the lithium ion diffusion coefficients.

Compared with layered LiCoO₂ and LiNiO₂ (Choi et al 1995), here in this work, the lithium ion diffusion coefficients of LiNi_{1/3}Co_{1/3}Mn_{1/3}O₂ cathode material are higher and vary in a small range with different lithium

intercalation states. This gives a clue to the better electrochemical performance of this LiNi_{1/3}Co_{1/3}Mn_{1/3}O₂ cathode material synthesized by normal high-energy ball milling method. We believe that the citric acid added in the milling process plays a crucial role here. The chelating and polymerization effects between transition metal ions and organic molecules facilitate the homogeneous mixing of reacting components.

4. Conclusions

LiNi_{1/3}Co_{1/3}Mn_{1/3}O₂ cathode material synthesized by citric acid assisted high-energy ball milling shows high charge-discharge capacities and an excellent cycling performance. The lithium ion diffusion coefficients are determined by GITT method in the voltage range of 3.7–4.5 V. The results show that the lithium ion diffusion coefficients vary from 10⁻⁸ to 10⁻⁹ cm²·s⁻¹ and decrease with the increasing cell voltage during the charging process.

Acknowledgements

We gratefully acknowledge the support for this work from 973 fundamental research program from the Ministry of Science and Technology of China (grant number 2010CB635116), NSFC project 21173190, Educational Commission of Zhejiang Province (grant number Y201017390), Ningbo Science and Technology Bureau Project 2011A610086 and K C Wong Magna Fund in Ningbo University.

References

- Choi Y-M, Pyun S-I and Bae J-S 1995 *J. Power Sources* **56** 25
- Chuying O Y, Siqi S and Liquan C 2007 *J. Chinese Ceram. Soc.* **35** 89
- Dess E 2005 *Electrochim. Acta* **50** 2927
- Kobayashi H, Arachi Y and Emura S 2005 *J. Power Sources* **146** 640
- Lee K-M, Choi H-J and Lee J-G 2001 *J. Mater. Sci. Lett.* **20** 1309
- Li L, Tang X and Liu H 2010a *Electrochim. Acta* **56** 995
- Li Z, Du F and Bie X F 2010b *J. Phys. Chem. C* **114** 22751
- Lim S, Yoon C S and Cho J 2008 *Chem. Mater.* **20** 4560
- Luo X, Wang X and Liao L 2006 *J. Power Sources* **161** 601
- Shaju K M and Bruce P G 2006 *Adv. Mater.* **18** 2330
- Van der Ven A and Ceder G 2001 *J. Power Sources* **97** 529
- Wen C J, Huggins R A and Wepper W 1979 *J. Electrochem. Soc.* **126** 2258